

DESIGN CONSIDERATIONS AND PERFORMANCE EVALUATION OF A 6-kW, SINGLE-SWITCH, THREE-PHASE, HIGH-POWER-FACTOR, MULTI-RESONANT, ZERO-CURRENT-SWITCHING BUCK RECTIFIER

Yungtaek Jang and Milan M. Jovanović

DELTA Power Electronics Lab., Inc.
1872 Pratt Drive, Suite 1400
Blacksburg, VA 24060, USA

Abstract The paper provides a complete design procedure of the multi-resonant, zero-current-switched (ZCS), high-power-factor (HPF) buck rectifier for telecommunication applications and presents extensive experimental evaluations of its performance. The evaluation was performed on a 6-kW prototype operating from a $380\text{ V}_{(L-L,ms)} \pm 10\%$, three-phase input voltage. The evaluation results demonstrate that the input current shaping using the multi-resonant buck converter can be performed with a total harmonic distortion (THD) less than 5% and the maximum efficiency of 95%.

1. Introduction

In today's power electronics systems, three-phase bridge-rectifier circuits are commonly used for interfacing converter systems to three-phase ac sources. Generally, because of their discontinuous currents, bridge rectifiers increase the distribution current stress and decrease the power factor. In addition, they generate line-current harmonic distortions, which induce line-voltage distortions via the series impedance of the power system. Since these voltage harmonics may interfere with the operation of nearby loads, the limits on the allowable line current harmonic distortions have been imposed by various national and international agencies [1], [2].

Three-phase, high-power-factor (HPF), pulse-width-modulated (PWM) rectifiers based on the discontinuous-conduction mode (DCM) have been introduced and analyzed in [3] - [6]. Generally, these rectifiers have pulsating input currents and offer limited improvements of the total harmonic distortion (THD). The THD can be significantly improved by operating the rectifier in the continuous-conduction mode (CCM) [7]. Generally, the CCM implementations require six switches and a complex control. Due to a large number of switches, the cost of six-switch rectifiers is high. As a result, they are seldom used in lower-power applications.

Recently, a new single-switch, three-phase, HPF, multi-resonant, ZCS buck rectifier which operates in the

CCM has been introduced [8]. The major features of this rectifier are that both input and output currents are continuous and that high power factor and low-harmonic rectification is achieved naturally. In addition, in this rectifier, all semiconductor devices operate under soft-switching conditions. Specifically, the switch operates with zero-current turn-off, whereas the diodes operate with zero-voltage turn-on. Because of the ZCS of the switch, this circuit is suitable for the implementation with an IGBT.

In this paper, a complete design procedure of this rectifier for telecommunication applications and extensive experimental evaluations of its performance are presented. The evaluation was performed on a 6-kW prototype operating from a $380\text{ V}_{(L-L,ms)} \pm 10\%$, three-phase input voltage. The evaluation results show that the input current shaping using the multi-resonant buck converter can be performed with less than 5% THD at full output power, and at the nominal input voltage. In

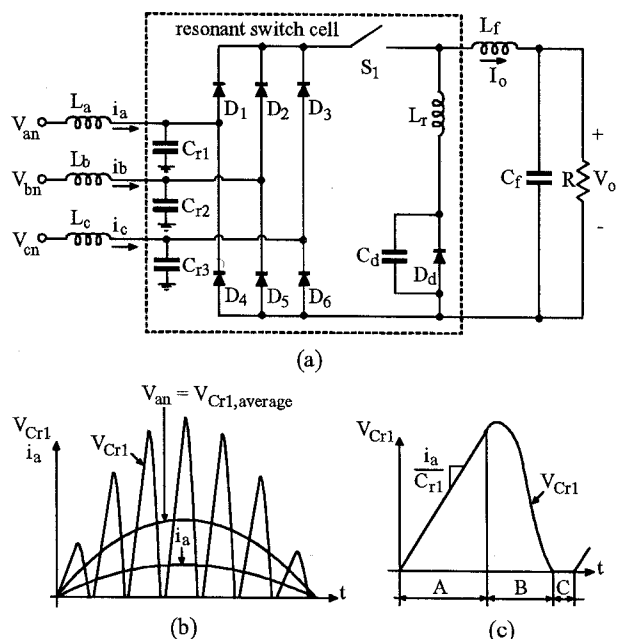


Fig. 1: (a) Three-phase, multi-resonant, ZCS cell, (b) the voltage waveform of resonant tank capacitor C_{r1} together with the input current waveform, and (c) the enlarged waveform of V_{Cr1} during one switching period.

addition, experimental results demonstrate that current harmonics of the input current satisfy the IEC555-2 standard over the entire input voltage and output power ranges. The maximum full load efficiency of the rectifier was measured as about 95%, while its approximate overall volume and weight are 6000 cm³ and 14 lb., respectively.

2. Review of Single-Switch, Multi-Resonant, ZCS, HPF Buck Rectifier [8]

2.1 Operation and Waveforms

Figure 1 shows the three-phase, multi-resonant, ZCS cell and the voltage wavelshape across input-side resonant capacitor C_r . Since input-filter inductors L_a , L_b , L_c , and output-filter inductor L_r are relatively large, they have small switching-frequency current ripples. In a steady state, the average voltage of C_r during a switching period is equal to the input voltage. Since the peak voltage of C_r is proportional to the input current, and switching frequency f_s is much higher than line frequency f_l , the input-current wavelshape follows the input-voltage wavelshape. As a result, the circuit possesses a high power factor and a low harmonic content in the input current.

In the circuit in Fig. 1, the amount of input-current distortions is dependent on the shape of the voltage waveform across C_r , shown in Fig. 1(c). During the first period when switch S_1 is off, V_{Cr} is increasing linearly with a slope proportional to input current i_a . During the second period when switch S_1 is on, resonant capacitor C_r resonates with inductor L_r until V_{Cr} reaches zero voltage. Finally, V_{Cr} remains at zero for the third period during which switch S_1 is still on. Since V_{Cr} is proportional to input current i_a only during the off time of switch S_1 , the input-current wavelshape becomes more proportional to the input-voltage waveform if the first period is longer than the sum of the second and the third periods. Because in the multi-resonant scheme in Fig. 1 the durations of the second and third periods are significantly reduced, the circuit performs the rectification with a low total harmonic distortion (THD).

2.2 Normalized control characteristic and stresses

To simplify the three-phase input and single-ended output circuit shown in Fig. 1(a), one operating point at

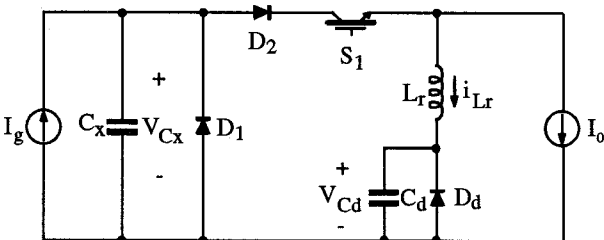


Fig. 2: The simplified single input and single output model of the single-switch, three-phase, multi-resonant, ZCS, HPF buck rectifier.

the time $\pi/2$ of the angular line frequency is chosen [8]. At this moment, phase voltage V_{an} is at its peak value, whereas phase voltages V_{bn} and V_{cn} are both negative and equal in magnitude to one-half of V_{an} . Since capacitors C_{r2} and C_{r3} shown in Fig. 1(a) are charged and discharged exactly in the same manner at this condition, capacitors C_{r2} and C_{r3} can be considered as parallel-connected capacitors. Also, phase current i_{an} is at its peak value, while i_{bn} and i_{cn} are both equal to one half of the negative phase current i_{an} . Therefore, the input-voltage sources and the input-filter inductors can be replaced by current source I_g , where I_g is peak phase current $i_{an-peak}$. Input-side resonant capacitors C_{r1} - C_{r3} can be replaced by an effective capacitor C_x which is equal to the series connection of C_{r1} and parallel connected C_{r2} and C_{r3} . Finally, the simplified single input circuit diagram is shown in Fig. 2. Diodes D_1 and D_2 of Fig. 2 represent the three phase input bridge diodes. The output filter inductor is replaced by current source I_o . The relations between the actual three phase input circuit and normalized quantities are described approximately by:

- $C_x = C_r \times 2/3$, where resonant capacitors C_{r1} - C_{r3} have the same values and are represented as C_r ,
- $I_g = \text{peak phase current } i_{an-peak}$
- $V_g = 3/2 \text{ times peak phase voltage } V_{an-peak}$,
- input power $P_{in} = V_g \times I_g = 3/2 \times (V_{an-peak} \times i_{an-peak})$.

The normalizing base quantities V_o , I_o , R_o , and f_o are defined as:

V_o — base voltage,

$I_o = V_o/R_o$ — base current,

$R_o = \sqrt{L_r/C_x}$ — characteristic impedance,

$f_o = 1/(2\pi\sqrt{L_r C_x})$ — base frequency,

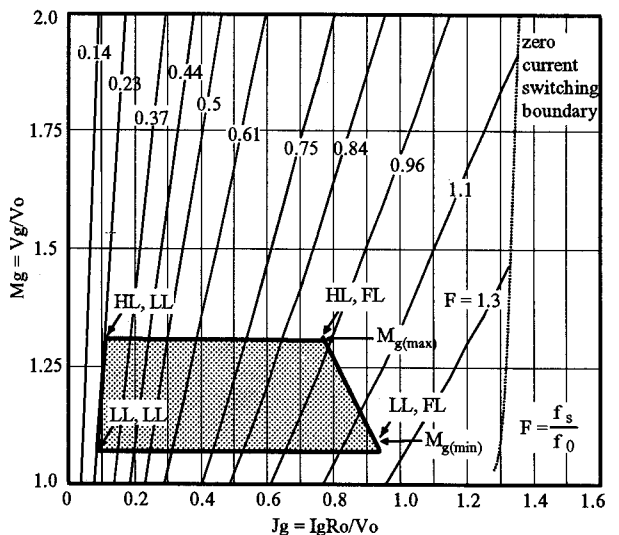
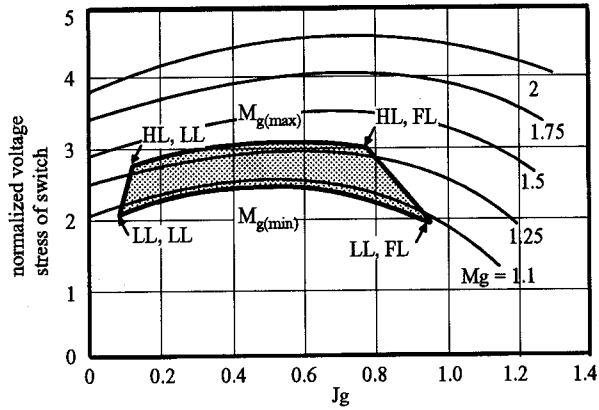
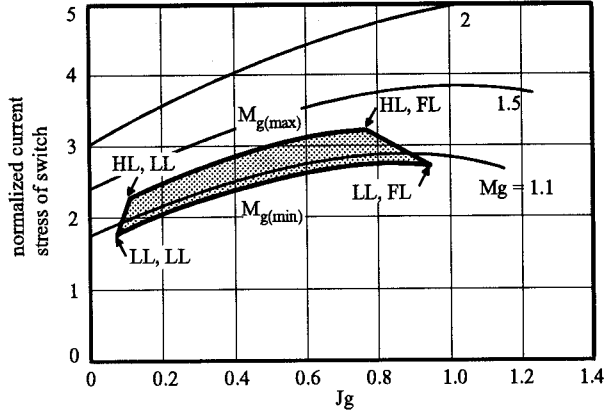


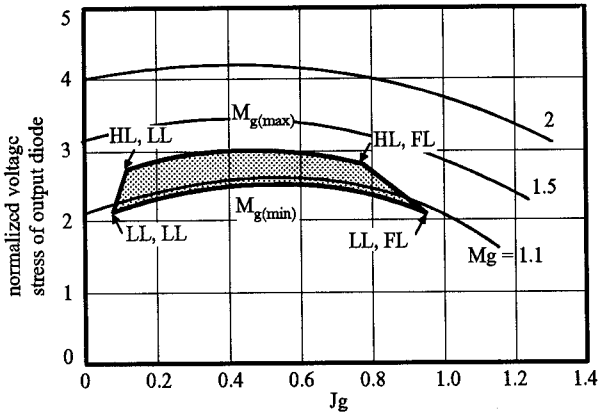
Fig. 3: The normalized input characteristic of the multi-resonant ZCS buck rectifier. The normalized frequency F is defined as the ratio of the switching frequency f_s and the resonant frequency f_o . The hatched area is the operating area for the experimental 6 kW converter presented in Section 3.



(a)



(b)



(c)

Fig. 4. Normalized stresses of the multi-resonant buck rectifier; (a) voltage stress of switch S_1 , (b) current stress of switch S_1 , and (c) voltage stress of output diode D_4 . The hatched area is the operating area for the experimental 6 kW converter presented in Section 3.

where V_o is the output voltage of the rectifier. Therefore, the normalized values of the input and output quantities are:

$$\text{normalized input voltage } M_g = V_g/V_o,$$

$$\text{normalized input current } J_g = I_g R_o/V_o,$$

$$\text{normalized output current } J_o = I_o R_o/V_o = M_g J_g.$$

Figure 3 shows the input characteristic of the converter, *i.e.*, normalized input current J_g vs. normalized input voltage M_g , for normalized switching

frequency $F = f_s/f_0$ as a parameter [8]. Figure 3 is indispensable in determining the converter's steady-state operating point and design parameters. It should be noted that the converter equations are normalized with respect to the dc output voltage instead of the ac input voltage. This allows the system waveforms to be expressed as functions of the dc operating point. The hatched area in Fig. 3 is the operating area for the experimental 6 kW converter presented in Section 3.

Figure 4 shows the normalized voltage stress and the normalized current stress of switch S_1 and output diode D_4 at different operating conditions. It should be noted that for a given output voltage the peak stresses occurs at the maximum input voltage. The current stress of the output diode is approximately equal to the output current.

3. Design of 6-kW Rectifier

3.1 Specifications

Input:

- Voltage V_{in} : 3-phase, 3-Wire System, $380 V_{(L-L,rms)} \pm 10\%$
- Line Frequency f_L : 47 - 63 Hz
- THD: < 5%
- Power Factor: > 0.98

Output:

- Voltage V_o : $400 V_{dc} \pm 2\%$ (0 - 100% load)
- Current I_o : 15 A
- Ripple Voltage: < $12.5 V_{peak-peak}$ (300/360 Hz)

Cooling:

- Force Convection

3.2 Design of Power and Control Circuits

From the specifications, effective input voltage $V_g =$

$$\frac{3}{2} \times V_{an-peak} = \frac{3}{2} \times \frac{380\sqrt{2}}{\sqrt{3}} = 465.4 \text{ V, and, hence,}$$

normalized nominal input voltage $M_{g(nom)} = V_g/V_o =$

$$465.4/400 = 1.16. \text{ From Fig. 3, normalized input current}$$

$J_{g(max)}$ is chosen to be 0.85 for the maximum output

power of 6 kW. The selection of $J_{g(max)}$ allows for more

than a 20% margin from the zero-current-switching

(ZCS) boundary ($J_g \approx 1.2$), which ensures the ZCS

operation in the entire input-voltage range

($380 V \pm 10\%$). Since at the maximum output power

$M_{g(nom)} = 1.16$ and $J_{g(max)} = 0.85$, normalized full-load

frequency F_{FL} is determined from Fig. 3 as $F_{FL} = 1.02$.

Furthermore, because output current $I_o = P_{out}/V_o = 15$ A

and output power $P_o \approx 6$ kW, the characteristic

impedance is $R_o = M_{g(nom)} J_{g(max)} V_o/I_o = 1.16 \times 0.85 \times 400/15$

$= 26.4 \Omega$, where $R_o = J_o V_o/I_o$ and $J_o = M_{g(nom)} J_{g(max)}$. If

the switching frequency at the full load of 6 kW is chosen

to be $f_{s(max)} = 87$ kHz, then resonant frequency f_0 can

be calculated as $f_0 = f_{s(max)}/F_{FL} = 87/1.02 = 85.3$ kHz. The

minimum switching frequency which occurs at the

minimum load (10% of the full load) is $f_{s(min)} = f_0 \times F_{LL} =$

$85.3 \times 0.23 = 20$ kHz, because at 10% of the full load

$J_{g(min)} = J_{g(max)}/10 = 0.085$ so that from Fig. 3, normalized

light-load frequency $F_{LL} = 0.23$. The operating region

for this design is indicated as a shaded area in Fig. 3. Four salient points which define the operating region are high-line full-load (HL, FL), low-line full-load (LL, FL), high-line light-load (HL, LL), and low-line light-load (LL, LL). The maximum normalized input voltage $M_{g(\max)}$ is 1.28 at input-voltage of $380 V_{\text{rms}} + 10\%$ and the minimum normalized input voltage $M_{g(\min)}$ is 1.06 at input-voltage of $380 V_{\text{rms}} - 10\%$.

The calculated effective capacitance C_x is $C_x = 1/(2\pi R_0 f_0) = 71 \text{ nF}$, whereas the resonant inductor inductance is $L_r = R_0/(2\pi f_0) = 49 \text{ }\mu\text{H}$. Therefore, input-side resonant capacitors C_{d1} - C_{d3} are $C_x = C_r \times 2/3 = 106.5 \text{ nF}$ and the value of output-side resonant capacitor C_d is chosen to be $C_x = C_d = 71 \text{ nF}$. This choice leads to a good compromise between low voltage stress and low input-current harmonics.

Since the peak voltage and the peak current stresses occur at the maximum input voltage of $456 V_{(L-L, \text{ms})}$ and full power of 6 kW, *i. e.*, for $M_{g(\text{HL, FL})} = 1.28$, $J_{g(\text{HL, FL})} = 0.77$. From Fig. 4(a), the peak value of the normalized voltage stress of switch S_1 for $M_{g(\text{HL, FL})} = 1.28$ and $J_{g(\text{HL, FL})} = 0.77$ is 3.1. Hence, the peak switch voltage is $V_{S1} = M_{S1} \times V_0 = 3.1 \times 400 \text{ V} = 1240 \text{ V}$. Similarly, from Fig. 4(b), the peak value of the normalized current stress of switch S_1 for $M_{g(\text{HL, FL})} = 1.28$ and $J_{g(\text{HL, FL})} = 0.77$ is 3.2 so that the peak switch current is $I_{S1} = J_{S1} \times V_0/R_0 = 3.2 \times 400 / 26.4 = 48.5 \text{ A}$. Finally, from Fig. 4(c), the peak value of the normalized voltage stress of output diode D_d for $M_{g(\text{HL, FL})} = 1.28$ and $J_{g(\text{HL, FL})} = 0.77$ is 3, *i. e.*, the peak output-diode voltage is $V_{Dd} = M_{Dd} \times V_0 = 3 \times 400 = 1200 \text{ V}$. The current stress of the output diode is equal to the output current, *i. e.*, 15 A.

Due to the wide input-voltage and load ranges, the closed-loop control of the prototype rectifier is implemented by a combination of a variable- and constant-frequency control. The circuit is controlled by the frequency control for the output power in the range from 6 kW to 600 W. In this power range the switching

frequency varies from 87 kHz at full power to 20 kHz at 10% of the load. When the output power falls below 600 W at the nominal input voltage, the constant frequency PWM control takes over.

Since for operation conditions when the constant-frequency PWM control is active, or during line and load transients, the switch operates with “hard” switching, the passive clamp circuit, shown in Fig. 5, is used to prevent any voltage overshoots. In fact, if the switch is turned off while a certain amount of current is flowing through it, the switch current is diverted through diodes D_{16} and D_{17} and clamping capacitor $C_{23} = 33 \text{ nF}$. During the next cycle, when the switch is turned on, diodes D_{14} and D_{15} conduct and recharge clamping capacitor C_{23} through inductor $L_4 = 1 \text{ }\mu\text{H}$. Because in the constant-frequency PWM control mode the output power is low, the clamping circuit operates with negligible losses.

3.3 Details of Selected Components

Semiconductors

The peak voltage stress on the switch is approximately 1240 V as shown in Section 3.2. The peak current, which is equal to sum of the peak tank inductor current and the output load current is approximately 49 A at full load. To reduce the current, two IGBTs, S_1 and S_2 (IXYS, IXSH 35N140A, $V_{\text{CBS}} = 1400 \text{ V}$, $I_{\text{C90}} = 35 \text{ A}$, $V_F = 3.4 \text{ V}$), were used in parallel in this prototype. These IGBTs do not have anti-parallel diodes since they are not necessary.

Since, the input bridge diodes must block 1240 V and must conduct a peak current of 49 A, two diodes (IXYS, DSEI 30-10 A, $V_{\text{RRM}} = 1000 \text{ V}$, $I_{\text{FAVM}} = 30 \text{ A}$, $t_{\text{tr}} = 35 \text{ ns}$) connected in series were used in each leg of the rectifier. Two capacitors (WIMA, FKP1 220 pF 1600 Vdc/500 Vac) were connected in parallel with these diodes for transient voltage sharing. Therefore, a

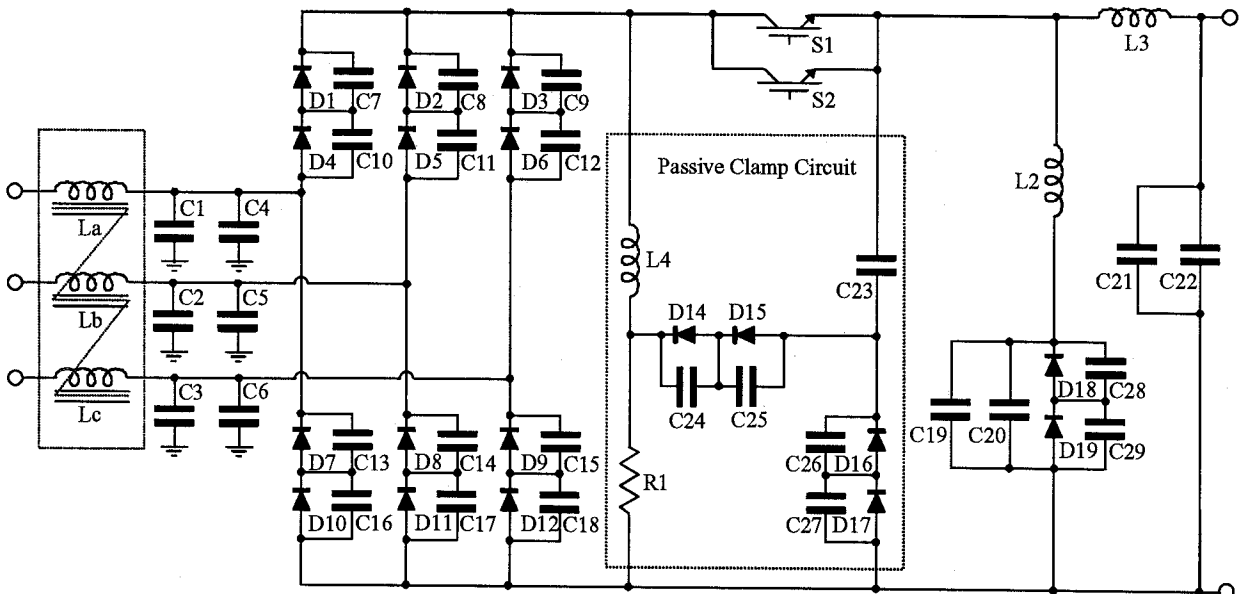


Fig. 5: Prototype circuit diagram of the 6-kW, three-phase, single-switch, multi-resonant, ZCS buck rectifier.

total of twelve diodes, $D_1 - D_{12}$ were used in this prototype for the input bridge rectifier. Also, because the output diode must block the same peak voltage as the output-side resonant tank capacitor voltage, or approximately 1200 V, and must conduct the output load current, or approximately 15 A, two diodes D_{18} and D_{19} (IXYS, DSEI 30-10 A, $V_{RRM} = 1000$ V, $I_{FAVM} = 30$ A, $t_{\pi} = 35$ ns) connected in series were used. Two capacitors C_{28} and C_{29} (WIMA, FKP1 220 pF 1600 Vdc/500 Vac) were connected in parallel with the diodes for transient voltage sharing.

Capacitors

High voltage polypropylene capacitors, with values of 0.1 uF and 0.033 uF, were used in parallel for the input-side tank capacitors. Two capacitors, with values of 0.033 uF and 0.047 uF, connected in parallel, were used for the output-side tank capacitor. The total values of the input- and output-side tank capacitors of 133 nF and 80 nF, respectively, are larger than calculated values shown in Section 3.2. This is a more conservative design which results in more margin from the zero-current-switching boundary. The followings are the specifications of the capacitors used on the circuit.

resonant capacitors :

$$C_1 = C_2 = C_3 = 0.1 \text{ uF (WIMA, FKP1 1600 Vdc/500 Vac)}$$

$$C_4 = C_5 = C_6 = 0.033 \text{ uF (WIMA, FKP1 1600 Vdc/500 Vac)}$$

$$C_{19} = 0.047 \text{ uF (WIMA, FKP1 1600 Vdc/500 Vac)}$$

$$C_{20} = 0.033 \text{ uF (WIMA, FKP1 1600 Vdc/500 Vac)}$$

parallel capacitors :

$$C_7 - C_{18}, C_{24} - C_{27} = 220 \text{ pF (WIMA, FKP1 1600 Vdc/500 Vac)}$$

output capacitors :

$$C_{21} = 1 \text{ uF (Polypropylene, 450 Vdc)}$$

$$C_{22} = 470 \text{ uF (Electrolytic, 450 Vdc)}$$

Input filter inductor

The desired inductance of the input filter inductors L_a , L_b , and L_c is 0.9 mH for each phase. This value was chosen to obtain the full-load, line-current THD of approximately 5%. Line-current THD is inversely proportional to the values of these inductors. Figure 6 shows the top view of the 3- ϕ input filter inductor

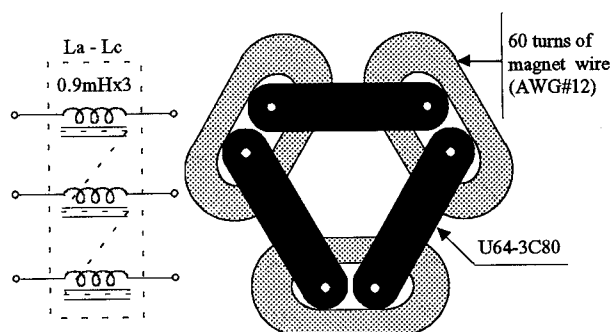


Fig. 6: Top view of the 3- ϕ input filter inductor.

construction. This structure doubles the utilization of the core material. Solid wire was used because the proximity effect is negligible at the line frequency. The input filters have the following specifications:

Core size: Three pairs of U64-3C80 ferrite cores (Three inductors are integrated as shown in Fig. 6).

Wire size: number of turns per phase = 60, magnet wire AWG #12.

Air gap size: 120×2 mils.

Resonant tank inductor

The desired inductance of the resonant tank inductor is 42.5 uH to obtain the desired resonant frequency of 85.3 kHz. Two sets of EE cores are used in parallel to reduce the flux density and number of turns of the winding. Litz wires were used to reduce the proximity effect of the winding. The resonant tank inductor has following specifications:

Core size: Two pairs of EE 65/32/27-3F3 ferrite cores.

Wire size: number of turns = 10, two Litz wires (1050 strands/AWG #42) in parallel.

Air gap size: 43×2 mils

Output filter inductor

The desired inductance of output filter inductor L_f is 0.8 mH. The output filter has the following specifications:

Core size: E80-3C85 ferrite cores

Wire size: number of turns = 85, magnet wire AWG #10.

Air gap size: 180×2 mils

Solid wire was used because the proximity effect is negligible.

Clamping circuit

Since the clamping diodes must be capable of blocking 1240V, two diodes, D_{14} and D_{15} , (IXYS, DSEI 30-10A, $V_{RRM} = 1000$ V, $I_{FAVM} = 30$ A, $t_{\pi} = 35$ ns) are connected in series. Two capacitors C_{24} and C_{25} (WIMA, FKP1 220 pF 1600 Vdc/500 Vac) are connected to the diodes for transient voltage sharing as shown in Fig. 5. Hence, four diodes $D_{14} - D_{17}$ and four capacitors $C_{24} - C_{27}$ were used for the clamping circuit in this prototype. The resonant frequency of L_4 and C_{23} is chosen to be 876 kHz, and hence one half of the resonant period becomes 0.57 usec, which is fast enough to recharge the clamping capacitor C_{23} during the switch-on period. The specifications of the clamp-circuit components are:

Clamping inductor :

$$L_4 = 1 \text{ uH}$$

(Core: MICROMETALS, T68-18A, iron powder core)

(Wire: PVC insulated single strand wire, AWG #18, 5 turns)

Clamping capacitor :

$$C_{23} = 0.033 \text{ uF (WIMA, FKP1 1600 Vdc/500 Vac)}$$

Clamping resistors :

$R_1 =$ three resistors (43 k Ω , 0.5 W) in series.

4. Experimental Results

The three-phase, single-switch, multi-resonant, ZCS buck rectifier as shown in Fig. 5 was built. The circuit's approximate overall volume is 6000 cm³ (power circuit ≈ 5000 cm³, control circuit ≈ 1000 cm³), and the approximate weight is 14 lb..

4.1 Efficiency and THD Measurements

Figure 7 shows the measured output power of the prototype rectifier at different switching frequencies. At a given input voltage, the output power of the rectifier is proportional to the switching frequency. Full load and 50% load operations are achieved at 90 kHz and 60 kHz switching frequencies, respectively.

The total harmonic distortion of the input-current of this rectifier as a function of the output power is shown in Fig. 8. Results demonstrate total harmonic distortion of less than 5% at full output power, less than 4% THD at 50% output power, and less than 2% THD at 10% output power with an EMI filter.

Figure 9 shows the measured efficiency of the rectifier. The rectifier efficiency is about 88% at 10% load and about 94.7% at full load.

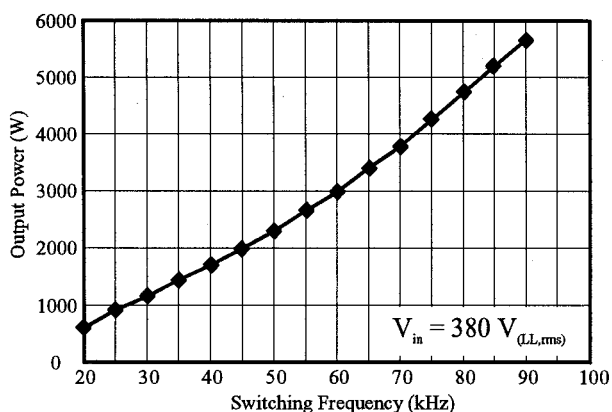


Fig. 7: Measured output power of the prototype rectifier at $V_{in} = 380 V_{(L-L, rms)}$.

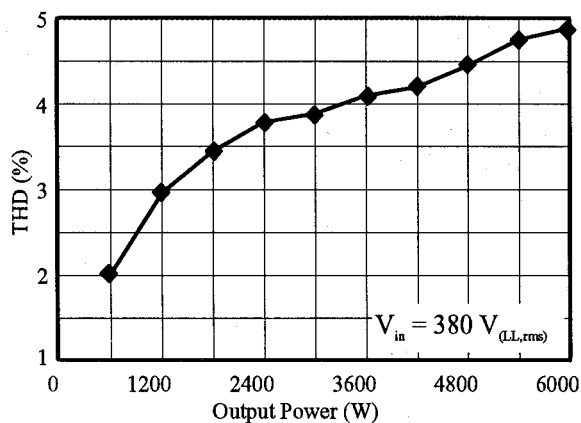


Fig. 8: Measured THD of the prototype rectifier as a function of the output power at $V_{in} = 380 V_{(L-L, rms)}$.

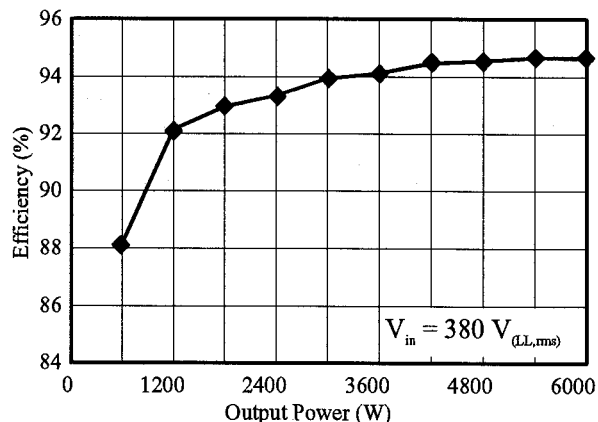


Fig. 9: Measured efficiency of the prototype rectifier as a function of the output power at $V_{in} = 380 V_{(L-L, rms)}$.

output power [kW]	peak switch voltage	peak diode voltage	peak switch current	peak diode current
6	1020 V	960 V	41 A	14.1 A
3	1020 V	900 V	37 A	7.4 A
0.6	1020 V	850 V	29 A	1.7 A

Table 1: Measured stresses of the switch and the output diode at different loads with input voltage 380 V_(L-L, rms).

Harmonic number	full load (6 kW)	50% load (3 kW)	10% load (600 W)	IEC555-2 limits
3	0.055 A	0.048 A	14 mA	2.3 A
5	0.363 A	0.147 A	5 mA	1.14 A
7	0.23 A	0.029 A	8 mA	0.77 A
9	0.018 A	0.006 A	0.5 mA	0.4 A
11	0.049 A	0.011 A	5.7 mA	0.33 A
2	0.025 A	0.012 A	1.3 mA	1.08 A
4	0.031 A	0.012 A	2.5 mA	0.43 A
6	0.013 A	0.002 A	0.27 mA	0.3 A
8	0.006 A	0.002 A	0.18 mA	0.23 A
10	0.013 A	0.003 A	0.27 mA	0.184 A
THD	4.82%	3.4%	2.0%	

Table 2: Measured current harmonics at different loads (The fundamental component of input current $I_{1, rms}$: 9.1 A at full load, 4.55 A at 50 % load, and 0.9 A at 10% load).

Table 1 shows the measured stresses of the switch and the output diode at three different load conditions, while Table 2 shows the measured rms harmonic content of the input current. The total harmonic distortion of the line current waveform is calculated numerically based on these measurements. The percentage of the total harmonic distortion was calculated for the first 98 harmonics (2nd ~ 99th). The measured rms harmonic currents of the line-input-current are compared with the harmonic limits of the

IEC555-2 regulations. The results show that these measured harmonics are under the IEC555-2 limits. Finally, Fig. 10 shows the measured efficiency of the rectifier at various input voltage conditions with the maximum load. The maximum efficiency of 94.7 % was obtained at the minimum input voltage.

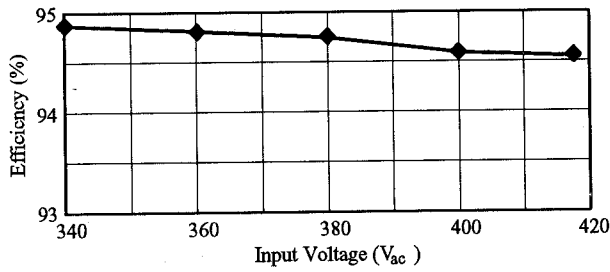


Fig. 10: Measured efficiency of the experimental rectifier as a function of the line voltage.

4.2 Key-Component Temperature Measurements

The temperature measurement of the prototype rectifier was performed at 6 kW output power and 380 V_(L-L, rms) input voltage. Results are shown in Table 3. The maximum temperatures of the IGBTs and the output rectifier diode are 58°C and 57.1°C, respectively, while the temperature of the resonant tank inductor copper and core is about 65°C. The maximum temperature of the input bridge rectifiers is 50.6°C. The ambient temperature was 29°C.

Devices	Temperature (°C)
IGBT 1	56.1
IGBT 2	58.0
Input Diode	50.6
Output Diode	57.1
Resonant Inductor (Wire)	63.2
Resonant Inductor (Core)	64.1

Table 3: Temperature measurements of the prototype rectifier with a cooling fan (15 W muffin fan).

4.3 Key Waveforms

The input current and the output voltage waveforms were measured at the start-up condition for 6 kW and 1 kW loads as shown in Figs. 11 and 12. Since buck-type rectifiers have a series switch between a source and its load, the start-up current control is much easier than boost-type rectifiers. Indeed, the experimental results show that the output voltage and the input current do not have significant overshoot. Moreover, the in-rush current at full output power complies with the specifications.

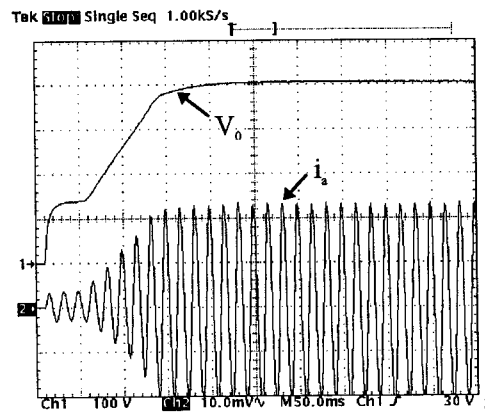


Fig. 11: Input current I_a (5 A/div) and output voltage V_o (100 V/div) measurements at a start-up condition with $V_{in} = 380 V_{(L-L, rms)}$ and $P_{out} = 6 kW$.

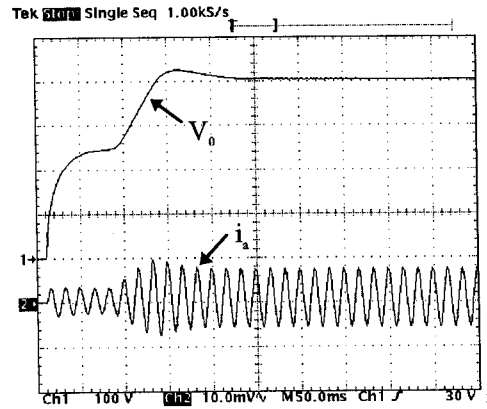


Fig. 12: Input current I_a (5 A/div) and output voltage V_o (100 V/div) measurements at a start-up condition with $V_{in} = 380 V_{(L-L, rms)}$ and $P_{out} = 1 kW$.

Figures 13 - 15 show the measured waveforms of the input line current of the prototype rectifier delivering 6 kW at three input voltages, $V_{in} = 340 V$, 380 V, and 417 V.

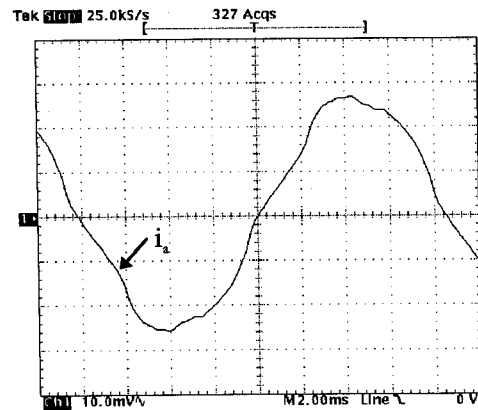


Fig. 13: Input current i_a waveform (5 A/div) at $V_{in} = 340 V_{(L-L, rms)}$, THDs = 6.8%.

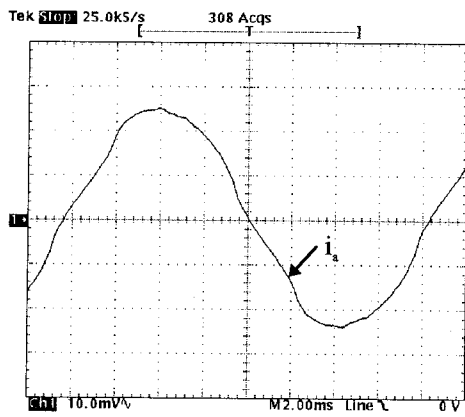


Fig. 14: Input current i_a waveform (5 A/div) at $V_{in} = 380 V_{(L-L, ms)}$, THDs = 4.82%.

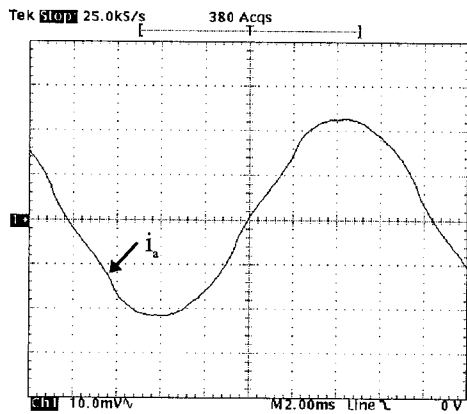


Fig. 15: Input current i_a waveform (5 A/div) at $V_{in} = 417 V_{(L-L, ms)}$, THDs = 4.1%.

5. Conclusion

In this paper, a complete design procedure of the multi-resonant, ZCS, HPF buck rectifier for telecommunication applications has been described. The experimental evaluation was performed on a 6-kW prototype operating from a $380 V_{(L-L, ms)} \pm 10\%$ three-phase input voltage. The evaluation results show that the input-current-shaping using the multi-resonant buck converter can be performed with less than 5% total harmonic distortion at full output power. In addition, the maximum efficiency of the front-end implementation with the multi-resonant buck converter is about 95% at full load. The measured rms harmonic currents of the line input current were well below the harmonic limits of the IEC555-2 regulations. The approximate overall volume and weight are 6000 cm^3 and 14 lb., respectively.

References

- [1] IEEE Std. 519-1992: IEEE Recommended practices and requirements for harmonic control in electrical power systems.
- [2] IEC Publication 555: Disturbances in supply systems caused by household appliances and similar equipment; Part 2: Harmonics.
- [3] A. R. Prasad, P. D. Ziogas and S. Manias, "An active power factor correction technique for three-phase diode rectifiers," IEEE Power Electronics Specialists Conference, 1989 Record, pp. 58 - 66.
- [4] E. H. Ismail and R. W. Erickson, "A single transistor three-phase resonant switch for high quality rectification," IEEE Power Electronics Specialists Conference, 1992 Record, pp. 1341 - 1351.
- [5] D. S. L. Simonetti, J. Sebastian and J. Uceda, "Single-switch three-phase power factor preregulator under variable switching frequency and discontinuous input current," IEEE Power Electronics Specialists Conference, 1993 Record, pp. 657 - 662.
- [6] J. W. Kolar, H. Ertl and F. C. Zach, "Space vector-based analytical analysis of the input current distortion of a three-phase discontinuous-mode boost rectifier system," IEEE Power Electronics Specialists Conference, 1993 Record, pp. 696 - 703.
- [7] H. Mao, D. Boroyevich, A. Ravindra, and F. C. Lee, "Analysis and Design of High Frequency Three-phase Boost Rectifiers," IEEE Applied Power Electronics Conference, 1996 Record, pp. 538 - 544.
- [8] Y. Jang and R. W. Erickson, "New single-switch three-phase high power factor rectifiers using multi-resonant zero current switching," IEEE Applied Power Electronics Conference, 1994 Record, pp. 711 - 717.